

# Implementation of a Novel Low-Cost Low-Profile Ku-Band Antenna Array for Single Beam Steering from Space

Nicholas K. Host, Chi-Chih Chen, John L. Volakis  
The Ohio State University  
The ElectroScience Laboratory  
Columbus, OH 43212

Félix A. Miranda  
NASA John Glenn Research Center  
Cleveland, OH 44135

**Abstract**—Phased array antennas afford many advantages over traditional reflector antennas due to their conformality, high aperture efficiency, and unfettered beam steering capability at the price of increased cost and complexity. This paper eliminates the complex and costly array backend via the implementation of a series fed array employing a propagation constant reconfigurable transmission line connecting each element in series. Scanning can then be accomplished through one small ( $\leq 100\text{mil}$ ) linear motion that controls propagation constant. Specifically, each element is fed via a reconfigurable coplanar stripline transmission line with a tapered dielectric insert positioned between the transmission line traces. The dielectric insert is allowed to move up and down to control propagation constant and therefore induce scanning. We present a 20 element patch array design, scanning from  $-25^\circ \leq \theta \leq 21^\circ$  at 13GHz. Measurements achieve only  $10.5^\circ \leq \theta \leq 22^\circ$  scanning due to a faulty, yet correctable, manufacturing process. Beam squint is measured to be  $\pm 3^\circ$  for a 600MHz bandwidth. This prototype was improved to give scanning of  $3.5^\circ \leq \theta \leq 22^\circ$ . Cross-pol patterns were shown to be -15dB below the main beam. Simulations accounting for fabrication errors match measured patterns, thus validating the designs.

## I. INTRODUCTION

Phased array antennas have advantages over traditional reflector antennas for use on satellites due to their conformality, high aperture efficiency, and unfettered beam steering capability. However, this improvement comes at the price of cost and complexity. The majority of these challenges arise from the backend, where a complex feeding network is required to achieve scanning. As would be expected, with additional elements, more feeding circuitry is needed, implying even more complexity. Typical treatments to deal with the excessive complexity and cost are array thinning [1] and sub arraying [2]. However, both of these degrade performance and are only marginally effective in decreasing cost and complexity.

To reduce cost and complexity for arrays of all sizes, we propose a novel feeding technique to eliminate the entire array backend. Specifically, we propose a linear array fed by a single CPS transmission line. The propagation constant of the latter is controlled by moving up and down a trapezoidal dielectric wedge. As the wedge moves, scanning is achieved.

In [3] we employ a parallel plate transmission line with three layers (dielectric, air, dielectric). By reconfiguring the thickness of the air layer, the effective dielectric constant was altered to induce scanning. However, this approach suffered from a very sensitive propagation constant when air layer thickness was reconfigured leading to excessively restrictive prototype tolerances. Subsequently, measured patterns deviated significantly from the simulated ones.

In [4] we proposed a novel transmission line to give more control over the propagation constant. We used a reconfigurable slotted coplanar stripline (CPS) transmission line with a trapezoidal dielectric wedge positioned between the traces. With this configuration, the propagation constant was reconfigured through a single small ( $\leq 100\text{mil}$ ) linear motion. The profile of the taper can be constructed to control the propagation constant as desired. Thus, the propagation constant sensitivity can be lessened and prototype tolerances lifted.

Other approaches employ reconfigurable transmission lines to induce beam scanning [5-10]. One such approach is the use of a nonfoster circuit is at each element to realize true time delay at the expense of complexity and cost [5]. The most common approach is to use ferrite [6-8], which can be biased to change the electrical properties. However, use of ferrite adds excessive weight and puts an inherent cap on bandwidth. Fluidic transmission lines [9] have also been explored. This, however, is only marginally effective in inducing scanning. Finally, [10] uses a concept similar to ours by positioning a dielectric sheet close to a microstrip line in a corporate feeding scheme. But, this setup is bulky. By contrast, our approach offers a lightweight, simple, cost effective alternative.

## II. RECONFIGURABLE SLOTTED COPLANAR STRIPLINE

### A. Propagation Constant Reconfiguration

Effective beam steering is accomplished through proper design of the reconfigurable transmission line. Here, we employ a propagation constant reconfigurable transmission line in a series fed array topology to induce scanning without the traditional phased array backend. In [3] a reconfigurable parallel plate transmission line suffered from great propagation sensitivity, leading to degraded prototype results. [4]

introduced a novel reconfigurable slotted coplanar stripline (CPS) with a trapezoidal dielectric wedge positioned between the line traces (Figure 1) that gave much greater control over propagation constant (Figure 2). By lifting the array board (green), a different portion of the insert (blue) is exposed to the supported wave, thus reconfiguring the propagation constant.

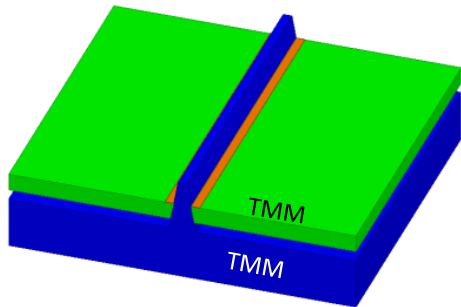


Figure 1. Reconfigurable slotted CPS transmission line achieved greater propagation constant control.

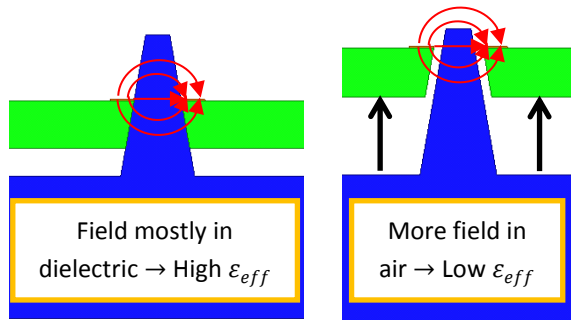


Figure 2. Trapezoidal dielectric wedge insert movement to control propagation constant. The profile of the tapered insert is shaped to give desired propagation control.

This varying propagation determines the progressive phase delivered to each element, thus inducing beam steering. As would be expected, the resulting scan angle is a function of both propagation constant and element spacing (Figure 3).

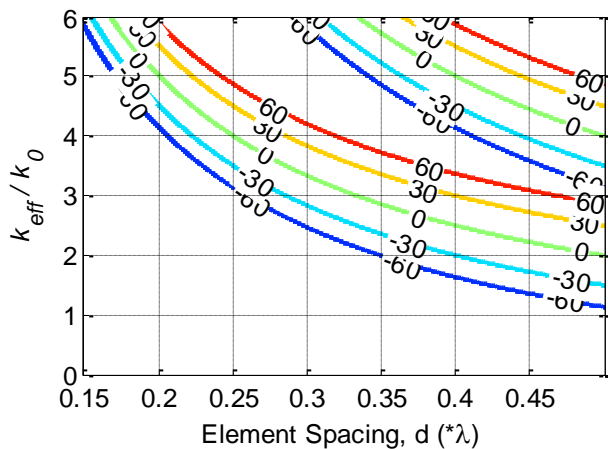


Figure 3. Scan angle from boresight as a function of propagation constant and element spacing.

### III. FINAL 20 ELEMENT PATCH ARRAY

#### A. Array Design and Performance

Achieving good control of the propagation constant is the goal in Figure 4. This design gave a nearly linear propagation constant to air gap,  $g$ , relationship. Impedance of the line is also favorable due to the relatively little change as  $g$  is reconfigured.

For the array, patches were chosen as the radiating elements due to several factors. The first is the strong radiation from patches and the second is related to the easily controllable impedance. This is important since, delivering equal amplitude excitation to each of the array elements requires an element impedance distribution along the transmission line of the array. Elements at the beginning of the line must be mismatched while elements at the end of the line must be well matched. This allows for most of the energy to continue down the line in the beginning with the remainder radiated at the end. Perfect distribution to every element is challenging to achieve due to varying line impedance during reconfiguration. However, good power distribution is achieved when impedance is tapered along the line.

A linear change in recess length (max at the first element and no recess on the last element) is used to give sufficient beamforming. Further optimization of scan patterns is possible. The array (see Figure 5) was designed to operate at 13GHz and scan from  $-25^\circ \leq \theta \leq 21^\circ$  (seen in Figure 6). A balun design from [11] was employed to feed the array.

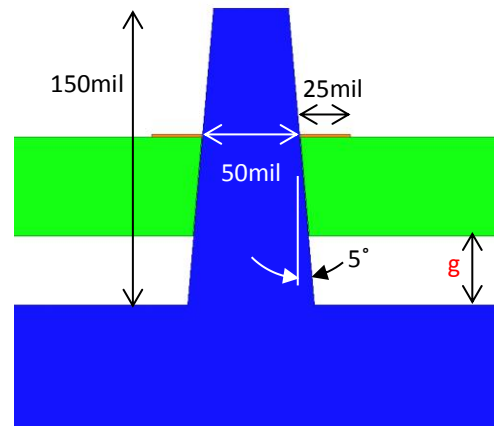


Figure 4. Reconfigurable slotted CPS transmission line giving  $\pm 30^\circ$  scan range while ensuring low propagation sensitivity (and thus non-restrictive prototype tolerances).

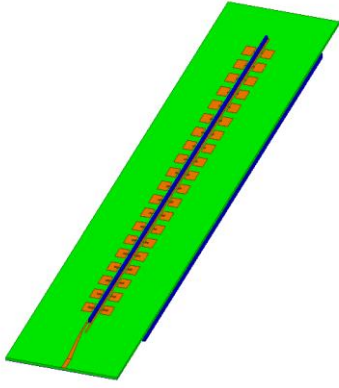


Figure 5. 20 element CPS patch array design employing a linear change in patch feed inset length along the array to ensure nearly uniform excitation.

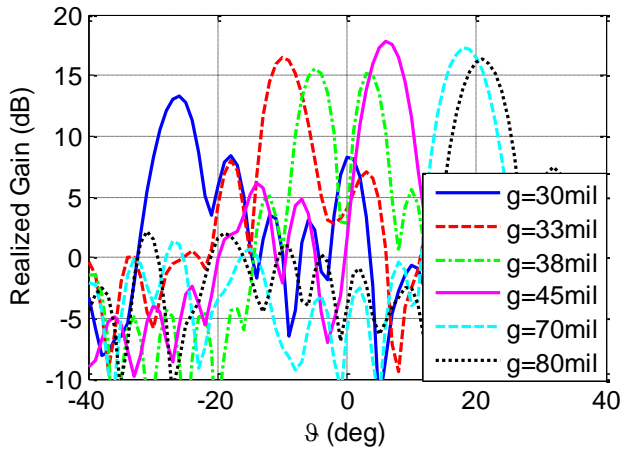


Figure 6. Simulated scan patterns for the CPS fed patch array demonstrating scanning in the range  $-25^\circ \leq \theta \leq 21^\circ$ .

### B. Prototype Measured Patterns

A prototype of the design was fabricated and tested. Unfortunately, during construction of the prototype, the array board was broken as pictured in Figure 7. The two pieces of the board were then glued back together and nylon rods were attached to give stability. For measurements, various  $g$  values were achieved with spacers, and binder clips were used rather than traditional clamps due to their consistent pressure applied. Warping of the board due to varying clamp pressures was found to be a problem during the parallel plate prototype testing, thus the use of binder clips was a simple solution.

Measured co-polarization patterns are depicted in Figure 8. Beam squint was about  $\pm 3^\circ$  for a high communications bandwidth of 600MHz at a gap of  $g=45\text{mil}$  as seen in Figure 9. Measured scan patterns deviate from the simulated in two ways; gain level and scan range. Gain level was reduced due to increased  $S_{11}$  from the board fracture (Figure 10). This was verified via a time domain  $S_{11}$  measurement as seen in Figure 11.

The decreased scan range ( $10.5^\circ \leq \theta \leq 22^\circ$ ) can be attributed to two factors as depicted in Figure 12. The first is the insert being machined to an angle of  $\alpha = 3.5^\circ$  rather than the design angle of  $\alpha = 5^\circ$ . The differing angle introduces

extra air since the array board and insert no longer fit together. This will eliminate some portion of the high propagation constant region and thus a portion of the scan range. Additionally, due to the differing angles, comparing the same gap,  $g$ , values in the two cases is no longer fair.

The second factor contributing to the reduced scan range is the recessing of the transmission line traces,  $R = 2\text{mil}$ , from the slot edge. The extra air introduced in the gap between the line traces and the slot edge also decreases the achievable scan range. The lines were recessed from the slot edge due to the poorly executed photolithography process. Instead of the traces extending fully to the slot edge, the edges of the trace were etched away. This manufacturing error is easily correctable.

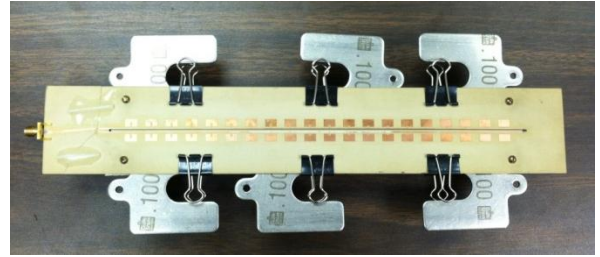


Figure 7. Assembled CPS prototype repaired with glue and nylon bracers after array board was broken during fabrication.

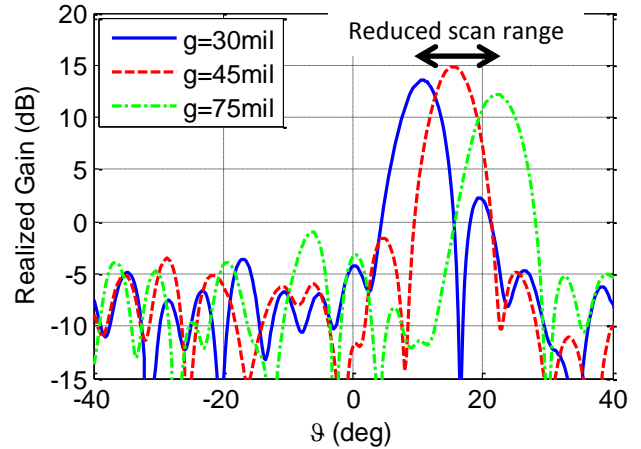


Figure 8. Measured scan patterns for the CPS fed prototype showing reduced gain and scan range.

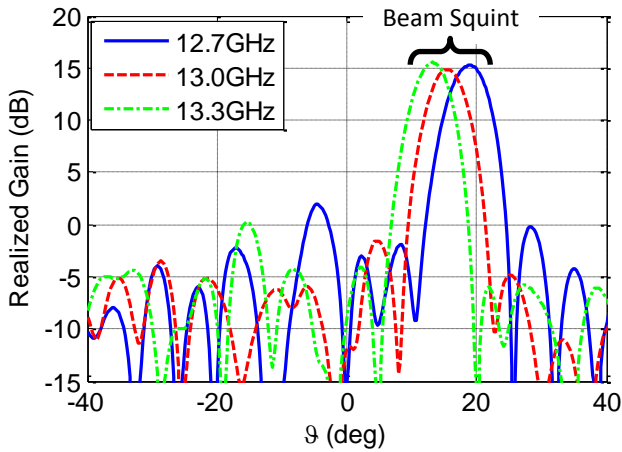


Figure 9. Measured scan patterns for the CPS fed prototype over a 600MHz bandwidth at  $g=45\text{mil}$  showing a beam squint of  $\pm 3^\circ$ .

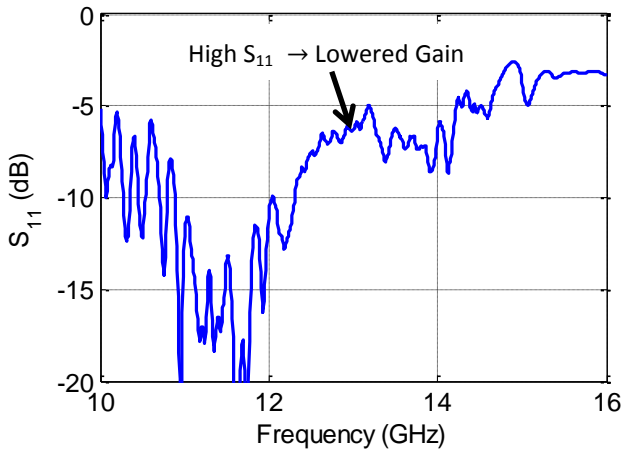


Figure 10. Measured  $S_{11}$  of  $g=45\text{mil}$ , showing a large reflection.

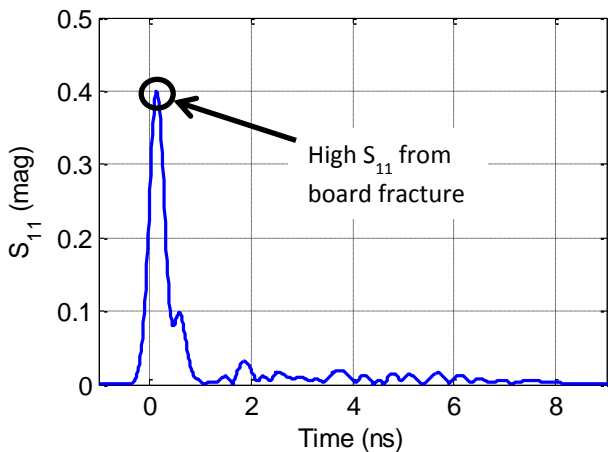


Figure 11. Measured time domain  $S_{11}$  of  $g=45\text{mil}$  with a large reflection seen at the board fracture location.

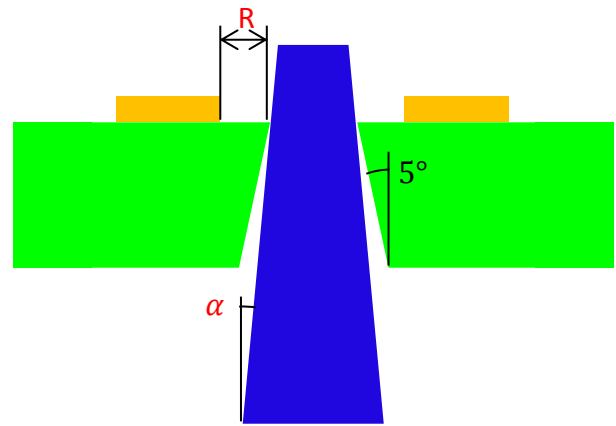


Figure 12. Errors in prototype Fabrication; recessed traces from slot edge ( $R$ ) leaving extra air, and the insert machined to the incorrect angle ( $\alpha$ ) also introducing extra air. This extra air eliminates the largest propagation constants achievable and thus scan range.

### C. Repairing the Array Using Silver Coating

Silver paint was applied to fill the air gap between the CPS traces and slot edge (as seen in Figure 13) to correct the photolithography error. Figure 14 now shows the measured scan patterns with the silver coating. As seen, the scanning range is increased to  $3.5^\circ \leq \theta \leq 22^\circ$ . Additionally, Figure 15 shows the cross-pol  $-15\text{dB}$  below co-pol in the main beam. However, the scan range is far from the ideal ( $-25^\circ \leq \theta \leq 21^\circ$ ) and gain is further reduced for all scan angles.

Though the exact conductivity of the silver coating is not known, measurements showed the silver paint was lossy. That is, the silver paint did not operate as intended. The majority of current density continued to travel through the recessed traces rather than the resistive silver painted surface. Therefore, scan range increased only slightly. Further, as would be expected, the lossy silver paint decreased the gain for all scan angles.

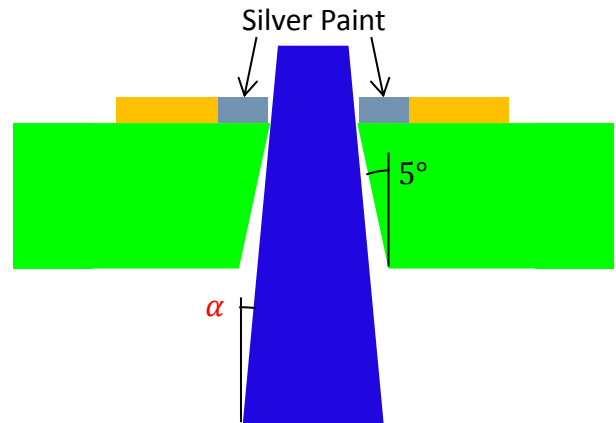


Figure 13. Silver coating added to correct the CPS line traces.

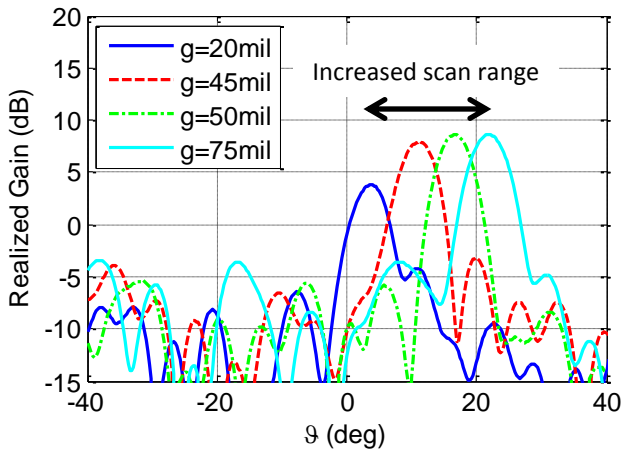


Figure 14. Measured scan patterns of CPS prototype with silver paint increasing scan range but reducing gain due to the lossy nature of the silver paint.

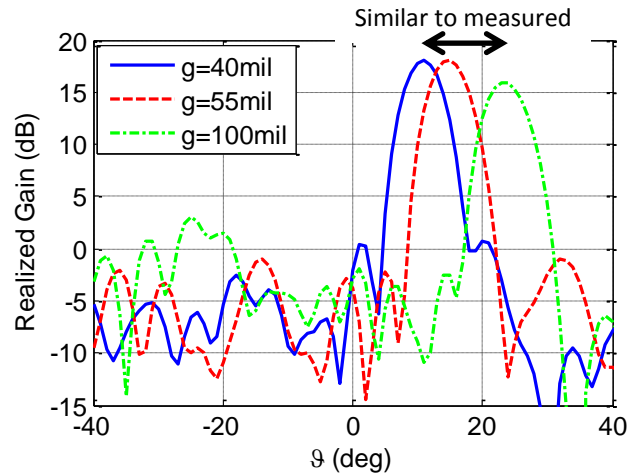


Figure 15. Simulated result of array with  $\alpha = 3.5^\circ$  and  $R = 2mil$  (to match the fabricated array) showing much better match to measurements.

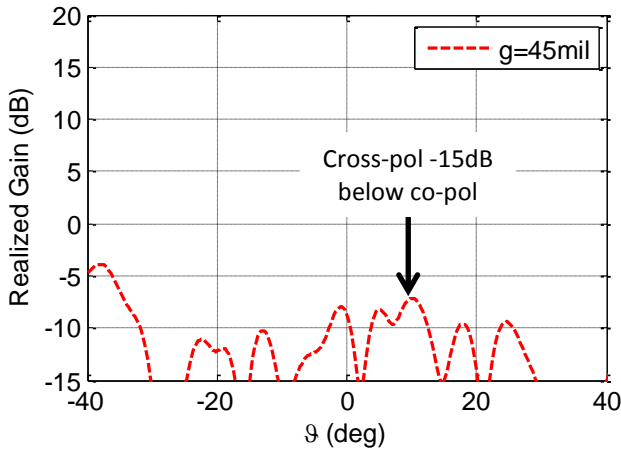


Figure 15. Cross-polarization pattern for  $g=45mil$  of the silver painted array -15dB below co-polarization in the main beam.

#### D. Simulated Effect of Fabrication Errors

The design was simulated with  $\alpha = 3.5^\circ$  and  $R = 2mil$ , to match the prototype parameters, as seen in Figure 15. These simulated patterns much better match the measured patterns and thus give validation to the simulations. Gain is still reduced due to the broken board, however, the scan range is almost identical.

These results bring up the question of which error has the larger effect. Figure 16 shows the array with  $\alpha = 5^\circ$  and  $R = 2mil$  while Figure 17 shows the array with  $\alpha = 3.5$  and  $R = 0mil$ . The insert angle was found to have much less of an effect than the recessed traces. This is expected considering the most critical parameter for determining the propagation constant is the air to dielectric ratio within the line connecting the transmission line traces. Adding a total of 4mils of air between the traces had a large effect. Changing the angle of the insert still allows the area between the traces to be completely filled with dielectric (at a smaller min gap,  $g = 16.7mil$ , rather than  $g=30mil$ ). With the insert angle, the scanning range is somewhat reduced due to the air introduced in the surrounding areas, but the critical region remains mostly unaffected.

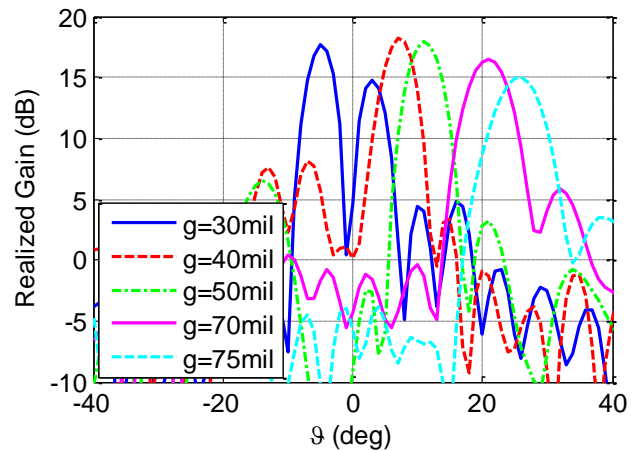


Figure 16. Simulated array with  $\alpha = 5^\circ$  and  $R = 2mil$  (only recessed trace error).



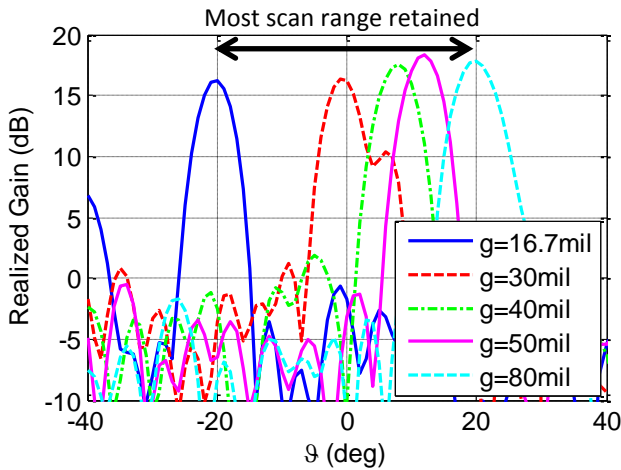


Figure 17. Simulated array with  $\alpha = 3.5^\circ$  and  $R = 0\text{mil}$  (only insert angle error).

#### IV. CONCLUSION

The implementation of a novel low cost, low profile, phased array feeding topology was presented. A propagation constant reconfigurable slotted CPS transmission line employed in a series fed array topology is employed in order to replace the traditional phased array backend. Scanning is accomplished via one small ( $\leq 100\text{mil}$ ) linear motion reconfiguring the propagation constant.

A slotted CPS transmission line design was presented allowing scanning to  $\pm 30^\circ$  while not requiring restrictive tolerances. The line was employed in a 20 element patch array operating at 13GHz. This array achieves a scan range of  $-25^\circ \leq \theta \leq 21^\circ$  with nearly uniform gain.

A prototype was fabricated and tested giving a scan range of  $10.5^\circ \leq \theta \leq 22^\circ$ , beam squint of  $\pm 3^\circ$  for a 600MHz bandwidth, and gain level 3dB below expected. Measured  $S_{11}$  revealed a large reflection from a board fracture incurred during fabrication, reducing measured gain. Scan range was reduced due to two manufacturing errors, insert angle and trace recess from slot edge. Silver paint was used in attempt to remedy the recessed traces. However, due to the lossy nature of the silver paint, scan range was only increased to  $3.5^\circ \leq \theta \leq 22^\circ$  and gain was further reduced. Cross-polarization patterns were -15dB below co-polarization patterns in the main beam. Finally, simulations revealed recessed traces were more critical to scan range than insert angle and thus should be the larger concern.

Future work will scale up the design to Ka band, consistent with satellite communications. This will bring the challenge of smaller features. Challenging prototype tolerances have already been encountered at 13GHz (and overcome in this paper) and will become even more restrictive at Ka band. Additionally, 2-D independent scanning will be accomplished

via an independent reconfigurable line feeding an array of reconfigurable linear arrays (all controlled together).

#### ACKNOWLEDGEMENT

This work was supported by a NASA Office of the Chief Technologist's Space Technology Research Fellowship (NSTRF), NASA Grant #NNX11AN16H. A special thanks to Ms. Elizabeth McQuaid (NASA GRC) and Dr. Kevin Lambert (Vantage Partners, LLC) for their help in the fabrication of the prototype and antenna metrology.

#### REFERENCES

- [1] Mosca, S.; Ciattaglia, M., "Ant colony optimization applied to array thinning," *Radar Conference, 2008. RADAR '08. IEEE*, vol., no., pp.1,3, 26-30 May 2008
- [2] Schrank, H.; Schuman, H., "Antenna Designer's Notebook-design curves for reducing the number of phase shifters in-phased arrays by subarraying," *Antennas and Propagation Magazine, IEEE*, vol.35, no.2, pp.56,58, April 1993
- [3] N. Host, C-C. Chen, J. Volakis, and F. Miranda, "Novel Phase Array Scanning Using Single Feed Without Using Individual Phase Shifters," 34<sup>th</sup> Annual Symposium of the Antenna measurement Techniques Association, Oct. 21-26, 2012 Bellevue, WA.
- [4] N. Host, C-C. Chen, J. Volakis, and F. Miranda, "Reconfigurable Transmission Line for a Series-Fed Ku-Band Phased Array Using a Single Feed," *IEEE Int. Symposium on Antennas and Propagation*, July 2013
- [5] Cherepanov, Andrei S.; Guskov, Anton B.; Yavon, Yu P.; Yufit, G.A.; Zaizev, E.F., "Innovative integrated ferrite phased array technologies for EHF radar and communication applications," *Phased Array Systems and Technology, 1996., IEEE International Symposium on*, vol., no., pp.74,77, 15-18 Oct 1996
- [6] Das, N.; Ray, A. K., "Magneto optical technique for beam steering by ferrite based patch arrays," *Antennas and Propagation, IEEE Transactions on*, vol.49, no.8, pp.1239,1241, Aug 2001
- [7] Ueda, T.; Yamamoto, S.; Kado, Y.; Itoh, T., "Pseudo-Travelling-Wave Resonator With Magnetically Tunable Phase Gradient of Fields and Its Applications to Beam-Steering Antennas," *Microwave Theory and Techniques, IEEE Transactions on*, vol.60, no.10, pp.3043,3054, Oct. 2012
- [8] Hui, W.W.G.; Bell, J.M.; Iskander, M.F.; Lee, J.J., "Low-Cost Microstrip-Line-Based Ferrite Phase Shifter Design for Phased Array Antenna Applications," *Antennas and Wireless Propagation Letters, IEEE*, vol.6, no., pp.86,89, 2007
- [9] Tang, Hongyan; Donnan, R.; Parini, C., "A novel phase shifter based patch antenna integrated electrostatic peristaltic micropumps," *Mobile Technology, Applications and Systems, 2005 2nd International Conference on*, vol., no., pp.4 pp., 15-17 Nov. 2005
- [10] Tae-Yeoul Yun; Kai Chang, "A low-cost 8 to 26.5 GHz phased array antenna using a piezoelectric transducer controlled phase shifter," *Antennas and Propagation, IEEE Transactions on*, vol.49, no.9, pp.1290,1298, Sep 2001
- [11] Zhi Chang Zheng; Guo Qing Luo, "Design of a compact wideband balun between microstrip and coplanar stripline," *Microwave Workshop Series on Millimeter Wave Wireless Technology and Applications (IMWS), 2012 IEEE MTT-S International*, vol., no., pp.1,3, 18-20 Sept. 2012